3164 *Organometallics* **2004,** *23,* 3164−3176

Electron Transfer and Chemical Reactions Associated with the Oxidation of an Extensive Series of Mononuclear Complexes [M(CO)$_2$(κ^1-P-P)(κ^2-P-P)X] and Binuclear Complexes [{M(CO)$_2$(κ^2-P-P)X}$_2$(μ-P-P)] (M = Mn, Re; P-P = Diphosphine or Related Ligand; X = Cl, Br)

Alan M. Bond,*[,1] Ray Colton,[1] Adrian van den Bergen,[1] and Jacky N. Walter[2]

School of Chemistry, P.O. Box 23, Monash University, Victoria 3800, Australia, and
Department of Chemistry, La Trobe University, Bundoora, Victoria 3083, Australia

Received December 18, 2003

The electrochemical oxidation of an extensive series of *cis,mer*-M(CO)$_2$(κ^1-dpm)(κ^2-P-P)X (M = Mn, Re; dpm = Ph$_2$PCH$_2$PPh$_2$; P-P = dpm, Ph$_2$PCH$_2$CH$_2$PPh$_2$ (dpe), *o*-(Ph$_2$P)$_2$C$_6$H$_4$-(dpbz); X = Cl, Br) complexes has been investigated on both the voltammetric and bulk electrolysis time scales. At short time domains or low temperatures, the manganese complexes undergo a reversible one-electron oxidation to *cis,mer*-[Mn(CO)$_2$(κ^1-dpm)(κ^2-P-P)X]$^+$. These compounds isomerize under slow scan rate voltammetric conditions at room temperature to give *trans*-[Mn(CO)$_2$(κ^1-dpm)(κ^2-P-P)X]$^+$, which on even longer bulk electrolysis time scales slowly lose X$^-$ to form a reactive *trans*-[Mn(CO)$_2$(κ^2-dpm)(κ^2-P-P)]$^{2+}$ intermediate. In turn, this complex is reduced either at the electrode surface (X = Cl) or in a homogeneous chemical reaction (X = Br) to form *trans*-[Mn(CO)$_2$(κ^2-dpm)(κ^2-P-P)]$^+$, which is the final product observed under conditions of bulk electrolysis. In contrast, the first oxidation step for the corresponding rhenium complexes involves oxidation of the pendant phosphorus atom and reaction with traces of water to give *cis,mer*-Re(CO)$_2$(κ^1-dpmO)(κ^2-dpm)X and then *cis*-[Re(CO)$_2$(κ^2-dpmO)$_2$]$^+$, with the rhenium center subsequently being oxidized at more positive potentials. Methylation of the pendant phosphorus of *cis,mer*-Re(CO)$_2$(κ^1-dpm)(κ^2-dpm)X gives *cis,mer*-[Re(CO)$_2$(κ^1-dpmMe)(κ^2-dpm)X]$^+$. The ligand-based oxidation pathway is blocked by the methylation, so that only the usual metal-centered Re(I)/Re(II)-based oxidation processes are observed in the voltammetry of these compounds. The compounds *cis,mer*-Re(CO)$_2$(κ^1-ape)(κ^2-ape)X and *cis,mer*-[Re(CO)$_2$(κ^1-apeMe)(κ^2-ape)X]$^+$ (ape = Ph$_2$AsCH$_2$CH$_2$PPh$_2$) exhibit electrochemistry similar to that of the dpm analogues. The major products of the interaction of dpe with the metal pentacarbonyl halides (2:1) are the new binuclear species {M(CO)$_2$(κ^2-dpe)X}$_2$(μ-dpe), whose structures have been determined by IR and ^{31}P NMR spectroscopy and electrospray mass spectrometry (ESMS). The stereochemistry of the manganese complexes is *cis,fac*, and upon voltammetric oxidation, first one and then the second manganese atom are oxidized. Bulk oxidative electrolysis at low temperature leads to the generation of *cis,fac*-[{Mn(CO)$_2$(κ^2-dpe)X}$_2$(μ-dpe)]$^+$ and *cis,fac*-[{Mn(CO)$_2$(κ^2-dpe)X}$_2$(μ-dpe)]$^{2+}$. The stereochemistry of the oxidized metal centers isomerizes to *trans*$^+$ at room temperature, but the binuclear structure is retained. Bulk reductive electrolysis at low temperature after bulk oxidative electrolysis at room temperature leads to the characterization of *trans*-{Mn(CO)$_2$(κ^2-dpe)X}$_2$(μ-dpe). The binuclear rhenium complexes *cis,mer*-{Re(CO)$_2$(κ^2-P-P)X}$_2$(μ-P-P) (P-P = dpe, Ph$_2$P(CH$_2$)$_3$PPh$_2$ (dpp)) were isolated, and they each undergo two successive one-electron oxidations to generate the mono- and dications without any isomerization on the voltammetric time scale. ESMS provides independent proof of the binuclear nature of the oxidized species.

Introduction

The interactions of the group 7 metal carbonyl halides M(CO)$_5$X (M = Mn, Re; X = Cl, Br, I) with 1 mol equiv of a variety of diphosphines (P-P) have been investigated extensively and give exclusively *fac*-M(CO)$_3$(κ^2-P-P)X,[3−6] where subsequently the hapticity symbol, κ, is often omitted for simplicity for these and other compounds in which all the diphosphine ligands are bidentate. In contrast, reactions with 2 mol equiv of P-P give a range of dicarbonyl products which appear to be dependent

---

* To whom correspondence should be addressed. Fax: (61)(3) 9905 4597. E-mail: alan.bond@sci.monash.edu.au.

[1] Monash University.

[2] La Trobe University.

[3] Osborne, A. G.; Stiddard, M. H. B. *J. Chem. Soc.* **1962**, 4715.

[4] Reimann, R. H.; Singleton, E. *J. Organomet. Chem.* **1972**, *38*, 113.

[5] Edwards, D. A.; Marshalsea, J. *J. Organomet. Chem.* **1975**, *96*, C50.

[6] Colton, R.; McCormick, M. J. *Inorg. Chem.* **1977**, *16*, 155.

10.1021/om034388t CCC: $27.50

upon the identity of the ligand. Thus, Mn(CO)$_5$X is reported to react with dpm (dpm = Ph$_2$PCH$_2$PPh$_2$) to give *cis,mer*-Mn(CO)$_2$(κ^1-dpm)(κ^2-dpm)X,[7,8] while with dpe (dpe = Ph$_2$PCH$_2$CH$_2$PPh$_2$) the compounds *trans*-[Mn(CO)$_2$(κ^2-dpe)$_2$]X[9] have been prepared. Analogous products have been reported for rhenium.[10-12]

In this paper, we have synthesized manganese and rhenium dicarbonyl halides with a wide variety of diphosphine ligands. The dicarbonyl complexes prepared include further examples of the aforementioned monomeric types, together with new binuclear species. Extensive oxidative electrochemical studies on both voltammetric and bulk electrolysis time scales are described for all the species. The electrochemical studies reveal a wide range of reaction pathways for both the monomeric and dimeric dicarbonyl compounds, with the details depending on the metal (Mn or Re), the halide (Cl or Br), and the coordination mode of the diphosphine ligand. Compound characterization is achieved by a combination of IR and ^{31}P NMR spectroscopy, voltammetry, and electrospray mass spectrometry (ESMS).

Experimental Section

(i) Materials. All solvents used in synthetic procedures were distilled and dried analytical reagent grade, and all preparations utilized 100 mL volumes of refluxing solvent under a nitrogen atmosphere. Manganese and rhenium carbonyls and phosphine ligands (Strem) were used as supplied. The pentacarbonyl halides were prepared by interaction of the carbonyls with halogen.[13] Fac-M(CO)$_3$(κ^2-P-P)X (M = Mn, R; P-P = diphosphine or related ligand; X = Cl, Br) were prepared by reaction of equimolar quantities of M(CO)$_5$X (1 g) and ligand in refluxing chloroform for 2 h (manganese complexes) or toluene for 3 h (rhenium complexes). The solvent was removed under vacuum and the solid recrystallized from dichloromethane/hexane.

(ii) Preparation of Manganese Complexes. The known[7,8] complexes *cis,mer*-Mn(CO)$_2$(κ^1-dpm)(κ^2-dpm)X (X = Cl, Br) (structure I) were prepared by reacting 0.5−0.7 g of the tricarbonyl species *fac*-Mn(CO)$_3$(dpm)X with a 1:1 molar ratio of dpm in refluxing heptane for approximately 16 h. After the mixture was cooled, the liquid was decanted and the precipitate from this reaction was dissolved in dichloromethane and passed through a column of silica in order to remove any charged species present. Hexane was added to the eluted solution, which was cooled to 0 °C and left standing overnight. Orange crystals of *cis,mer*-Mn(CO)$_2$(κ^1-dpm)(κ^2-dpm)X precipitated from the solution and were collected by gravity filtration. IR and ^{31}P NMR spectra agree with literature values,[10,11] but the yields were found to be significantly higher (90−95%). The *trans*-[Mn(CO)$_2$(κ^2-dpe)$_2$]X and *trans*-Mn(CO)(κ^2-dpe)$_2$X (X = Cl, Br) complexes were synthesized by refluxing a mixture of 0.5−0.7 g of Mn(CO)$_5$X and dpe in a 1:2 molar ratio for 5−7 h in toluene. When the mixture was cooled to room temperature, *trans*-[Mo(CO)$_2$(κ^2-dpe)$_2$]X precipitated. Cooling to 0 °C and standing overnight resulted in crystallization of *trans*-Mn(CO)(κ^2-dpe)$_2$X. Spectroscopic data for these complexes agree with literature values. The mixed-diphosphine complexes Mn(CO)$_2$(κ^1-dpm)(κ^2-P-P)Br (P-P = dpe, dpbz; dpbz = *o*-(Ph$_2$P)$_2$C$_6$H$_4$) were prepared in a way similar to that for *cis,mer*-Mn(CO)$_2$(κ^1-dpm)(κ^2-dpm)X by the interaction of 0.7 g of *fac*-Mn(CO)$_3$(P-P)Br with a 1:1 molar mixture of dpm, except that a longer reflux time of 22 h was employed in refluxing heptane. Yields obtained were in the range of 90 ± 5%. Analogous reactions of 0.5−0.7 g of Mn(CO)$_5$X and dpe (1:2 molar ratio) yielded a mixture of compounds with a reflux time of 13 h for the chloro compounds and 22 h for the bromo compounds. After removal of the solvent, recrystallization from dichloromethane/hexane gave as the major product (85−90% yield) a solid which was characterized (next section) as orange needles of the binuclear complex *cis,fac*-{Mn(CO)$_2$(dpe)X}$_2$(μ-dpe). Evaporation of the filtrate and several recrystallizations from dichloromethane gave *cis*-Mn(CO)$_2$(κ^1-dpe)(κ^2-dpe)X as a minor product (≤5% yield).

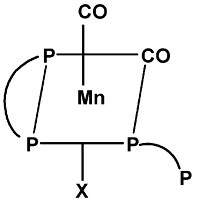

Structure I

(iii) Preparation of Rhenium Complexes. The complexes *cis,mer*-Re(CO)$_2$(κ^1-dpm)(κ^2-dpm)X (structure type I) were prepared by the literature method described for the chloro compound.[10] Thus, 0.5 g of Re(CO)$_5$XC and dpm (1:2 molar ratio) were refluxed in methylene for 6 h. However, the ^{31}P NMR spectra showed the presence of weak resonances in addition to those expected for *cis,mer*-Re(CO)$_2$(κ^1-dpm)(κ^2-dpm)X. A precipitate was collected by gravity filtration, washed with hexane, and air-dried. Passing a dichloromethane solution of the mixture of compounds through a silica column, followed by addition of hexane to the eluted solution, gave an 85 ± 5% yield of the pure complex *cis,mer*-Re(CO)$_2$(κ^1-dpm)(κ^2-dpm)X, obtained as a white solid. The impurity mentioned above was isolated by further elution of the silica column with acetone and subsequent removal of the solvent under vacuum (≤5% yield). It was characterized as the known[11] *cis,mer*-Re(CO)$_2$(κ^1-dpmO)(κ^2-dpm)X (structure II), previously generated by bubbling dry air through a solution of *cis,mer*-Re(CO)$_2$(κ^1-dpm)(κ^2-dpm)X. The known[10] complexes *cis,mer*-[Re(CO)$_2$(κ^1-dpmMe)(κ^2-dpm)X]I (structure III) were prepared in 85 ± 5% yield by the addition of (1.3:1 molar ratio) excess MeI to a dichloromethane solution of 0.5−0.7 g of *cis,mer*-Re(CO)$_2$(κ^1-dpm)(κ^2-dpm)X. The solution was allowed to stand overnight and the solvent then removed under vacuum. To investigate the electrochemical properties of the methylated cationic

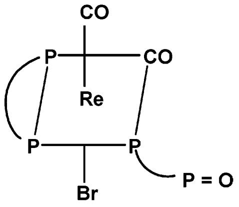

Structure II

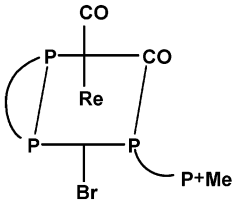

Structure III

---

(7) Carr, S. W.; Shaw, B. L.; Thornton-Pett, M. *J. Chem. Soc., Dalton Trans.* **1985**, 2131.

(8) Carriedo, G. A.; Riera, V.; Santamaria, J. *J. Organomet. Chem.* **1982**, *234*, 175.

(9) Osborne, A. G.; Stiddard, M. H. B. *J. Chem. Soc.* **1965**, 700.

(10) Carr, S. W.; Shaw, B. L.; Thornton-Pett, M. *J. Chem. Soc., Dalton Trans.* **1987**, 1763.

(11) Carriedo, G. A.; Rodriguez, M. L.; Garcia-Granda, S.; Aguirre, A. *Inorg. Chim. Acta*, **1990**, *178*, 101.

(12) Freni, M.; Valenti, V.; Guisto, D. *J. Inorg. Nucl. Chem.* **1965**, *27*, 2635.

(13) Colton, R.; McCormick, M. J. *Aust. J. Chem.* **1976**, *29*, 1657.

species, it was necessary to replace iodide by PF_6^-, since iodide is electrochemically active in the potential range of interest. This was undertaken by pretreatment of an anion exchange column with KPF_6 and passing an acetone solution of the methylated complex through the column. Reaction of 0.5−0.7 g of $Re(CO)_5X$ and dpe (1:2 molar ratio) in refluxing mesitylene for 5 h yielded 80 ± 5% of the binuclear complexes *cis,mer*-$\{Re(CO)_2(dpe)X\}_2(\mu$-dpe), whose characterization is given in the Results and Discussion. Upon cooling of the solution, a white solid precipitated which was then collected by filtration and washed with hexane. Reaction between 0.5 g of $Re(CO)_5X$ and dpe (1:2 molar ratio) under the milder conditions of refluxing xylene (4 h) yielded 90 ± 5% *cis,mer*-$Re(CO)_2(\kappa^1$-dpe)(κ^2-dpe)X after the precipitate formed on cooling was dissolved in dichloromethane and the solution chromatographed using a silica column and dichloromethane as the eluent. *cis,mer*-$Re(CO)_2(\kappa^1$-ape)(κ^2-ape)X (ape = $Ph_2AsCH_2CH_2PPh_2$) was prepared similarly. Additon of a 1:3:1 molar excess of MeI to a dichloromethane solution yielded *cis,mer*-[$Re(CO)_2(\kappa^1$-apeMe)(κ^2-ape)X]I after the solution was allowed to stand overnight and the solvent removed under vacuum. Despite extensive efforts, no crystals suitable for X-ray structural analysis could be obtained for any of the new compounds.

(iv) Electrochemical Methods. Dichloromethane (HPLC grade) was pretreated with alumina to remove any acid impurities. Dichloromethane (electrolyte) solutions gave satisfactory blank voltammograms. Conventional voltammetric measurements typically were obtained with 1.0 mM solutions of compound in dichloromethane (0.1 M Bu_4NPF_6), using a Cypress Systems (Lawrence, KS) Model CYSY-1 computer-controlled electrochemical system or a BAS 100A electrochemical analyzer (Bioanalytical Systems, West Lafayette, IN). The working electrode was a glassy-carbon disk (0.5 mm radius), the auxiliary electrode was a platinum wire, and the reference electrode was Ag/AgCl (saturated LiCl in dichloromethane (0.1 M Bu_4NPF_6)) separated from the test solution by a salt bridge. The reversible voltammetry of an approximately 1.0 mM ferrocene (Fc) solution in the same solvent was used as a reference redox couple, and all potentials are quoted relative to Fc^+/Fc. Near steady-state voltammograms were recorded using a 12.5 μm radius platinum-microdisk electrode. Solutions were purged with solvent-saturated nitrogen before voltammetric measurements and then maintained under an atmosphere of nitrogen during the measurements.

Bulk electrolysis experiments were undertaken in dichloromethane with 0.4 M Bu_4NPF_6 or 0.4 M Bu_4NclO_4 as the electrolyte with a BAS 100 A electrochemical analyzer using a large platinum basket working electrode, a platinum-gauze auxiliary electrode separated from the test solution by a salt bridge, and the same reference electrode as used in the voltammetric studies. Coulometric analysis of the bulk electrolysis data was used to either determine the purity of the compound or the *n* value of the electrode process if the purity had been established by independent methods.

(v) Spectroscopic Methods. ^1H and proton-decoupled ^{31}P and ^{13}C NMR spectra were recorded on a Bruker AM 300 spectrometer (^{31}P at 121.496 MHz in dichloromethane and ^{13}C at 75.469 MHz in $CDCl_3$ solution). The high-frequency-positive convention is used for chemical shifts with external 85% H_3PO_4 (^{31}P) and internal TMS (^1H and ^{13}C) references. Infrared spectra were recorded on Perkin-Elmer FT-IR 1720X and Perkin-Elmer 1430 IR spectrometers.

(vi) Electrospray Mass Spectrometry, Positive ion electrospray mass spectra were obtained with a VG Bio-Q triple quadrupole mass spectrometer using a water/methanol/acetic acid (50:50:1) mobile phase. Solutions of the compounds (2.0 mM in dichloromethane) were mixed, if necessary, with oxidant or sodium acetate, as described in the text. The mixed solution then was diluted 1:10 with methanol and immediately injected directly into the spectrometer via a Rheodyne injector fitted with a 10 μL loop. A Pheonix 20 micro LC syringe pump delivered the solution to the vaporization nozzle of the electrospray source at a flow rate of 5 μL min^{-1}. Nitrogen was used as the drying gas and for nebulization with flow rates of approximately 3 L min^{-1} and 100 mL min^{-1}, respectively. The voltage on the first skimmer (B1) was usually 40 V, but higher voltages were used to induce collisionally activated fragmentations as described in the text. Peaks are identified by the most abundant mass in the isotopic mass distribution.

(vii) Analysis of Solids. Elemental analysis and proton NMR spectra of the compounds, with a few exceptions, demonstrated that solvent obtained from the refluxing solvent and/or solvent used for recrystallization or even MeI (when relevant) was present. Attempts to fully remove solvent by heating altered the solvent component but did not completely remove solvent, according to elemental analysis, and/or caused decomposition, except in the cases of $Mn(CO)_2(\kappa^1$-dpm)(κ^2-dpe)Br, $Mn(CO)_2(\kappa^1$-dpe)(κ^2-dpe)Br, and $Re(CO)_2(\kappa^1$-dpe)(κ^2-dpe)Br. In studies on the related $Re(CO)(dpe)_2Br$ compound, where an X-ray structure was obtained, molecular modeling of the crystal structure[14] revealed the presence of hydrophobic channels that are believed to enable ready uptake of organic solvents and formation of material with widely variable solvent composition. A similar situation is believed to prevail with many of the compounds prepared in this study. Elemental microanalyses for compounds prepared and recrystallized from different solvents were performed by Chemsearch, University of Otago, Otago, New Zealand, and provided the following representative data where 0, 0.5, 0.75, 1.0, and 1.5 mol of dichloromethane are present from recrystallization from this solvent. Anal. Found (calcd) for $[Mn(CO)_2(dpe)_2]Br\cdot0.5CH_2Cl_2$: C, 63.7 (63.5); H, 4.9 (4.8). Found (calcd) for $Mn(CO)_2(\kappa^1$-dpm)(κ^2-dpb)$Br\cdot0.75CH_2Cl_2$: C, 64.8 (64.5); H, 3.7 (3.5). Found (calcd) for $Mn(CO)_2(\kappa^1$-dpm)(κ^2-dpe)Br: C, 65.0 (65.4); H, 5.0 (4.8). Found (calcd) for $Mn(CO)_2(\kappa^1$-dpe)(κ^2-dpe)Br: C, 62.5 (62.5); H, 4.6 (4.7). Found (calcd) for $Re(CO)_2(\kappa^1$-dpe)(κ^2-dpe)Br: C, 54.1 (54.2); H, 3.9 (4.0). Found (calcd) for $Re(CO)_2(\kappa^1$-dpe)(κ^2-dpe)$Br\cdot1.5CH_2Cl_2$: C, 53.0 (53.5); H, 4.1 (4.4). Found (calcd) for $Re(CO)_2(\kappa^1$-dpm)(κ^2-dpm)$Br\cdot CH_2Cl_2$: C, 54.4 (54.2); H, 4.2 (3.9). Found (calcd) for [$Re(CO)_2(\kappa^1$-dpmMe)(κ^2-dpm)Br]$I\cdot0.5CH_2Cl_2$: C, 50.4 (50.7); H, 3.7 (3.8).

In view of the difficulty of obtaining solvent-free samples for microanalysis or crystals suitable for X-ray structural characterization, mass spectral data for new compounds having the expected *m/z* values have been obtained (Tables 1 and 2). Importantly, in all cases, the agreement between experimental and theoretical isotropic mass patterns was excellent. ^{13}C and ^1H NMR data obtained for deuterated acetonitrile solutions revealed the presence of dichloromethane, chloroform, MeI, or refluxing solvent as appropriate in most of the samples. However, ^{31}P NMR data for dichloromethane solutions of the compounds prepared by chemical means or by bulk electrolysis (see later; Figures S1−S7, Supporting Information) showed no evidence of phosphine ligand or any other diamagnetic phosphine-containing impurities. Data obtained by NMR and IR (Tables 3 and 4) are fully consistent with the structures reported (see Results and Discussion). Voltammetric analysis was used to confirm the presence or absence (<0.1%) of free halide or phosphine. In the case of the binuclear complexes, where variable solvent composition of between 0.15 and 0.65 mol of solvent/mol of complex was obtained on the basis of microanalysis data, quantitative coulometric analysis confirmed that the purity used for electrochemical and spectroscopic examination was 97 ± 1.5%, assuming that the oxidation process employed for this purpose was a 1.0 or 2.0 electron oxidation process (see below). Further details of the characterization of all compounds are contained in section A of the Results and Discussion.

---

(14) Snook, G. A.; Bond, A. M.; Fletcher, S. *J. Electroanal. Chem.* **2003**, *554*−555, 157.

Table 1. Electrospray Mass Spectrometric Data for Manganese Complexes

compd	additive	ion	*m/z*
fac-Mn(CO)$_3$(dpe)Br	NaOAc	[Na + Mn(CO)$_3$(dpe)Br]$^+$	641
		[Mn(CO)$_3$(dpe)]$^+$	537
cis,mer-Mn(CO)$_2$(κ^1-dpm)(κ^2-dpm)Br	NaOAc	[Na + Mn(CO)$_2$(dpm)$_2$Br]$^+$	983
		[Mn(CO)$_2$(dpmO)(dpm)]$^+$	895
		[Mn(CO)$_2$(dpm)$_2$]$^+$	879
cis,mer-Mn(CO)$_2$(κ^1-dpm)(κ^2-dpm)Br		[H + Mn(CO)$_2$(dpm)$_2$Br]$^+$	961
cis,mer-Mn(CO)$_2$(κ^1-dpm)(κ^2-dpm)Cl		[H + Mn(CO)$_2$(dpm)$_2$Cl]$^+$	983
		[Mn(CO)$_2$(dpmO)(dpm)]$^+$	895
		[Mn(CO)$_2$(dpm)$_2$]$^+$	879
trans-[Mn(CO)$_2$(dpm)$_2$]PF$_6$[a]		[Mn(CO)$_2$(dpm)$_2$]$^+$	879
cis-Mn(CO)$_2$(κ^1-dpm)(κ^2-dpe)Br		[H + Mn(CO)$_2$(dpm)(dpe)Br]$^+$	975
cis-Mn(CO)$_2$(κ^1-dpm)(κ^2-dpbz)Br		[H + Mn(CO)$_2$(dpm)(dpbz)Br]$^+$	1023
		[Mn(CO)$_2$(dpmO)(dpbz)]$^+$	957
		[Mn(CO)$_2$(dpm)(dpbz)]$^+$	941
trans-[Mn(CO)$_2$(dpe)$_2$]Br		[Mn(CO)$_2$(dpe)$_2$]$^+$	907
cis,fac-{Mn(CO)$_2$(dpe)Cl}$_2$(μ-dpe)	NOBF$_4$	[Mn$_2$(CO)$_2$(dpe)$_3$Cl$_2$]$^+$	1488
cis,fac-{Mn(CO)$_2$(dpe)Br}$_2$(μ-dpe)	NOBF$_4$	[Mn$_2$(CO)$_2$(dpe)$_3$Br$_2$]$^+$	1576
		[Mn$_2$(CO)$_2$(dpe)$_3$Br$_2$]$^{2+}$	788

[a] From exhaustive electrolysis of *cis,mer*-Mn(CO)$_2$(κ^1-dpm)(κ^2-dpm)X.

Table 2. Electrospray Mass Spectrometric Data for Rhenium Complexes

compd	additive	ion	*m/z*
c,m-[Re(CO)$_2$(κ^1-dpmMe)(κ^2-dpm)Cl]PF$_6$		[Re(CO)$_2$(dpmMe)(dpm)Cl]$^+$	1061
		[dpmMe]$^+$	399
		[Ph$_2$P=CH$_2$]$^+$	199
cis,mer-Re(CO)$_2$(κ^1-dpm)(κ^2-dpm)Br	NaOAc	[Na + Re(CO)$_2$(dpm)$_2$Br]$^+$	1113
c,m-[Re(CO)$_2$(κ^1-dpmMe)(κ^2-dpm)Br]PF$_6$		[Re(CO)$_2$(dpmMe)(dpm)Br]$^+$	1105
cis-[Re(CO)$_2$(dpmO)$_2$]ClO$_4$		[Re(CO)$_2$(dpmO)$_2$]$^+$	1043
c,m-[Re(CO)$_2$(κ^1-apeMe)(κ^2-ape)Cl]PF$_6$		[Re(CO)$_2$(apeMe)(ape)Cl]$^+$	1177
		[apeMe]$^+$	457
		[Ph$_2$P=CH$_2$]$^+$	199
cis,mer-Re(CO)$_2$(κ^1-ape)(κ^2-ape)Br		[H + Re(CO)$_2$(apeO)(ape)Br]$^+$	1223
		[H + Re(CO)$_2$(ape)$_2$Br]$^+$	1207
c,m-[Re(CO)$_2$(κ^1-apeMe)(κ^2-ape)Br]PF$_6$		[Re(CO)$_2$(apeMe)(ape)Br]$^+$	1221
cis,mer-Re(CO)$_2$(κ^1-dpm)(κ^2-dpe)Br	NaOAc	[Na + Re(CO)$_2$(dpm)(dpe)Br]$^+$	1127
cis,mer-{Re(CO)$_2$(dpe)Cl}$_2$(μ-dpe)	NaOAc	[Na + {Re$_2$(CO)$_4$(dpe)$_3$Cl$_2$}]$^+$	1773
cis,mer-{Re(CO)$_2$(dpe)Cl}$_2$(μ-dpe)	NOBF$_4$	[Re$_2$(CO)$_3$(NO)(dpe)$_3$Cl$_2$]$^+$	1752
		[Re$_2$(CO)$_4$(dpe)$_3$Cl$_2$]$^+$	1750
cis,mer-{Re(CO)$_2$(dpe)Br}$_2$(μ-dpe)	NaOAc	[Na + {Re$_2$(CO)$_4$(dpe)$_3$Br$_2$}]$^+$	1863
cis,mer-{Re(CO)$_2$(dpe)Br}$_2$(μ-dpe)	NOBF$_4$	[Re$_2$(CO)$_3$(NO)(dpe)$_3$Br$_2$]$^+$	1840
		[Re$_2$(CO)$_4$(dpe)$_3$Br$_2$]$^+$	1838
cis,mer-{Re(CO)$_2$(dpp)Br}$_2$(μ-dpp)	NOBF$_4$	[Re$_2$(CO)$_4$(dpp)$_3$Br$_2$]$^+$	1882
		[Re$_2$(CO)$_4$(dpp)$_3$Br]$^+$	1801

Table 3. IR (Carbonyl Region) and ^{31}P NMR Data in Dichloromethane for Manganese Complexes Obtained from Synthesized Compounds or from Bulk Electrolysis Experiments

compd	ν(CO) (cm^{-1})	δ(^{31}P) (ppm)	temp (NMR) (°C)
cis,mer-Mn(CO)$_2$(κ^1-dpm)(κ^2-dpm)Cl	1940, 1867	52.9, 36.6, 1.7, −28.6	22
trans-Mn(CO)$_2$(κ^1-dpm)(κ^2-dpm)Cl	1892	56.2, 51.5, 19.7, −31.6	−40
trans-[Mn(CO)$_2$(κ^1-dpm)(κ^2-dpm)Cl]$^+$	1976		
cis,mer-Mn(CO)$_2$(κ^1-dpm)(κ^2-dpm)Br	1937, 1867	50.3, 35.0, 0.3, −28.1	22
trans-Mn(CO)$_2$(κ^1-dpm)(κ^2-dpm)Br	1891	53.2, 49.3, 19.0, −31.8	−40
trans-[Mn(CO)$_2$(κ^1-dpm)(κ^2-dpm)Br]$^+$	1972		
trans-[Mn(CO)$_2$(dpm)$_2$]$^+$	1916	35.3	22
cis-Mn(CO)$_2$(κ^1-dpm)(κ^2-dpe)Br	1939, 1867	81.4, 53.0, 47.5, −28.2	22
trans-Mn(CO)$_2$(κ^1-dpm)(κ^2-dpe)Br	1889	98.9, 75.1, 54.4, −29.9	−40
trans-[Mn(CO)$_2$(κ^1-dpm)(κ^2-dpe)Br]$^+$	1971		
cis-Mn(CO)$_2$(κ^1-dpm)(κ^2-dpbz)Br	1940, 1867	85.8, 61.1, 47.2, −28.3	22
trans-Mn(CO)$_2$(κ^1-dpm)(κ^2-dpbz)Br	1893	102.8, 86.5, 53.2, −30.0	−40
trans-[Mn(CO)$_2$(κ^1-dpm)(κ^2-dpbz)Br]$^+$	1972		
cis-Mn(CO)$_2$(κ^1-dpe)(κ^2-dpe)Cl	1937, 1863	81.7, 54.2, 52.8, −14.2	22
cis-Mn(CO)$_2$(κ^1-dpe)(κ^2-dpe)Br	1937, 1866	79.6, 52.9, 51.2, −13.8	22
trans-[Mn(CO)$_2$(dpe)$_2$]Cl	1897	71.6	22
trans-[Mn(CO)$_2$(dpe)$_2$]Br	1897	71.9	22
trans-Mn(CO)(dpe)$_2$Cl	1826	73.2	22
trans-Mn(CO)$_2$(dpe)$_2$Br	1824	77.6	22
cis,fac-{Mn(CO)$_2$(dpe)Cl}$_2$(μ-dpe)	1937, 1863	80.8 (1), 52.9 (2)	22
trans-{Mn(CO)$_2$(dpe)Cl}$_2$(μ-dpe)	1889	100.5, 76.7, 59.2	−60
c,f(t)-[{Mn(CO)$_2$(dpe)Cl}$_2$(μ-dpe)]$^+$	1969, 1937, 1863		
trans-[{Mn(CO)$_2$(dpe)Cl}$_2$(μ-dpe)]$^{2+}$	1969		
cis,fac-{Mn(CO)$_2$(dpe)Br}$_2$(μ-dpe)	1937, 1865	79.1 (1), 50.9 (2)	22
trans-{Mn(CO)$_2$(dpe)Br}$_2$(μ-dpe)	1897	99.0, 75.2, 57.8	−60
c,f(t)-[{Mn(CO)$_2$(dpe)Br}$_2$(μ-dpe)]$^+$	1965, 1937, 1865		
trans-[{Mn(CO)$_2$(dpe)Br}$_2$(μ-dpe)]$^{2+}$	1965		

Results and Discussion

A. Characterization of Compounds. (i) Manganese Complexes. ^{31}P NMR and IR spectroscopic data for all manganese complexes isolated are summarized in Table 3, as are data (where available) for compounds generated by bulk electrolysis. Figures S1−S4 (Supporting Information) contain ^{31}P NMR spectra of Mn complexes. The new mixed-diphosphine complexes Mn(CO)$_2$(κ^1-dpm)(κ^2-P-P)Br (P-P = dpe, dpbz; dpbz = *o*-(Ph$_2$P)$_2$C$_6$H$_4$) exhibit two carbonyl IR stretches, indi-

Table 4. IR Data (Carbonyl Region) and ^{31}P NMR Data (22 °C) in Dichloromethane for Rhenium Complexes Obtained from Synthesized Compounds or from Bulk Electrolysis Experiments

compd	ν(CO) (cm^{-1})	δ(^{31}P) (ppm)[a]
cis,mer-Re(CO)$_2$(κ^1-dpm)(κ^2-dpm)Cl	1938, 1858	9.5*, −21.1*, −27.9, −44.6
cis,mer-Re(CO)$_2$(κ^1-dpmO)(κ^2-dpm)Cl	1942, 1864	23.4, 6.8*, −21.8*,−43.0
cis,mer-[Re(CO)$_2$(κ^1-dpmMe)(κ^2-dpm)Cl]PF$_6$	1942, 1869	18.7, 10.5*, −21.7*, −48.2
cis,mer-Re(CO)$_2$(κ^1-dpm)(κ^2-dpm)Br	1941, 1862	5.3*, −24.2*, −28.1, −47.7
cis,mer-Re(CO)$_2$(κ^1-dpmO)(κ^2-dpm)Br	1943, 1867	23.9, 2.9*, −24.2*, −45.6
cis,mer-[Re(CO)$_2$(κ^1-dpmMe)(κ^2-dpm)Br]PF$_6$	1943, 1870	18.0, 5.1*, −25.6, −50.1
cis-[Re(CO)$_2$(dpmO)$_2$]$^+$	1931, 1845	66.5, 31.5
cis,mer-{Re(CO)$_2$(dpe)Cl}$_2$(μ-dpe)	1943, 1857	34.4*, 18.5, 6.5*
cis,mer-{Re(CO)$_2$(dpe)Br}$_2$(μ-dpe)	1943, 1860	31.4*, 15.3, 2.3*
cis,mer-{Re(CO)$_2$(dpp)Br}$_2$(μ-dpp)	1951, 1857	−2.3*, −11.7*, −22.0
cis,mer-Re(CO)$_2$(κ^1-dpe)(κ^2-dpe)Cl	1942, 1856	36.9*, 21.3, 7.4*, −12.3
cis,mer-Re(CO)$_2$(κ^1-dpe)(κ^2-dpe)Br	1943, 1862	33.3*, 17.6, 2.9*, −12.2
cis,mer-Re(CO)$_2$(κ^1-ape)(κ^2-ape)Cl	1936, 1853	38.4*, 8.4*
cis,mer-Re(CO)$_2$(κ^1-apeO)(κ^2-ape)Cl	1938, 1856	37.4*, 10.5*
cis,mer-[Re(CO)$_2$(κ^1-apeMe)(κ^2-ape)Cl]PF$_6$	1940, 1860	38.2*, 11.2*
cis,mer-Re(CO)$_2$(κ^1-ape)(κ^2-ape)Br	1941, 1859	35.8*, 4.0*
cis,mer-Re(CO)$_2$(κ^1-apeO)(κ^2-ape)Br	1942, 1861	34.7*, 5.7*
cis,mer-[Re(CO)$_2$(κ^1-apeMe)(κ^2-ape)Br]PF$_6$	1942, 1866	35.1*, 6.1*

[a] The asterisks indicate that these pairs of phosphorus atoms in each compound are strongly coupled (J = 170−185 Hz), indicating a mutually trans configuration.

cating a cis carbonyl geometry. The ^{31}P NMR spectra for all of these types of compounds show four resonances of equal integrated intensities (Figure S1), and in each case a signal is observed close to the resonance position for free dpm, thus indicating that dpm is the κ^1 ligand. However, since coupling details could not be observed, a distinction cannot be made between *cis,fac*- and *cis,-mer*-Mn(CO)$_2$(κ^1-dpm)(κ^2-P-P)Br, and therefore the compounds are referred to as merely cis in Table 3. The trans isomeric forms produced by bulk oxidative and reductive electrolysis sequences (see later) of the cis isomer exhibit (Table 3) a single carbonyl stretch and four ^{31}P NMR resonances of equal intensity (Figure S2), as expected for the trans configuration.

The IR spectrum of the major product from the interaction of Mn(CO)$_5$Br and dpe (1:2) shows two absorptions of equal intensities, indicating a *cis*-dicarbonyl configuration. The ^{31}P NMR spectrum shows two strong resonances at δ 79.1 and 50.9 ppm of integrated intensities 1:2 (Figure S3). As both of these signals are at much higher frequency than the resonance of free dpe, the spectrum clearly indicates that all of the phosphorus atoms are coordinated to the metal. However, the 1:2 intensity ratio is not consistent with any monomeric formulation and leads to the conclusion that the compound is a dpe-bridged binuclear species. ESMS (Table 1) measurements, described in detail later, confirm the binuclear nature of this compound with the empirical formula Mn$_2$(CO)$_4$(dpe)$_3$Br$_2$. The IR and NMR data fix the geometry as *cis,fac*, as shown in structure IV.

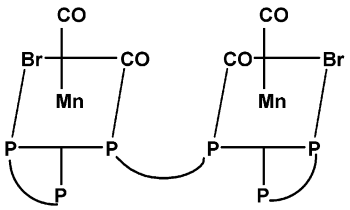

Structure IV

The minor product from the interaction of Mn(CO)$_5$Br and dpe (1:2) also shows two carbonyl stretches, again indicating a *cis*-dicarbonyl arrangement. The ^{31}P NMR spectrum consists of four signals of equal integrated intensities, one of which is close to the resonance of free dpe, which is consistent with the formulation Mn(CO)$_2$(κ^1-dpe)(κ^2-dpe)Br. Again, fine structure could not be discerned in the NMR spectrum of Mn(CO)$_2$(κ^1-dpe)(κ^2-dpe); therefore, these compounds also are referred to as merely *cis*-Mn(CO)$_2$(κ^1-dpe)(κ^2-dpe)X in Table 3. Details of the interpretation of spectra of compounds detected during the course of bulk electrolysis experiments (Table 3, Figure S4) are contained elsewhere in the text. The absence of ^{31}P coupling details in a number of cases could arise from line broadening associated with the presence of paramagnetic impurities. However, efforts to remove paramagnetic impurities by ion chromatography and bulk reductive electrolysis did not lead to changed spectra, and coupling also could not be detected at low temperatures.

(ii) Rhenium Complexes. Specroscopic data for the synthesized (^{31}P NMR and IR) and electrochemically generated rhenium complexes (IR) are summarized in Table 4. ^{31}P spectra of rhenium complexes are contained in Figures S5−S7 (Supporting Information). The ^{31}P NMR spectra of the complexes *cis,mer*-Re(CO)$_2$(κ^1-dpm)(κ^2-dpm)X consist of four resonances, two of which are coupled strongly, which indicates nonequivalent trans phosphorus atoms on rhenium, in agreement with the previously published data.[10] The ^{13}C NMR spectrum of a deuterated chloroform solution of *cis,mer*-Re(CO)$_2$(κ^1-dpm)(κ^2-dpm)Br shows two resonances in the carbonyl region, one of which appears as a doublet, which therefore is assigned to the carbonyl group trans to phosphorus. The IR spectrum of the compound shows the expected two carbonyl stretches, and all data are consistent only with the previously proposed structure.[10]

The IR spectrum of the impurity mentioned in the Experimental Section shows two stretches consistent with a *cis*-dicarbonyl geometry, and its ^{31}P NMR (Figure S5) spectrum shows four resonances of equal intensities. These are very similar to those previously reported[11] for *cis,mer*-Re(CO)$_2$(κ^1-dpmO)(κ^2-dpm)Br. Similar observations were made for the *cis,mer*-Re(CO)$_2$(κ^1-dpm)(κ^2-dpm)Cl system. The complexes *cis,mer*-[Re(CO)$_2$(κ^1-dpmMe)(κ^2-dpm)X]I were prepared by the addition of MeI to *cis,mer*-Re(CO)$_2$(κ^1-dpm)(κ^2-dpm)X, which methylates the pendant phosphorus atom to give the phosphonium salt. To investigate the electrochemical properties of the methylated cationic species, it was necessary to replace iodide by PF$_6^-$ by ion exchange, since iodide is electrochemically active in the potential range of interest. The IR spectrum of *cis,mer*-[Re(CO)$_2$(κ^1-dpmMe)(κ^2-dpm)Br]PF$_6$ shows two absorption bands very similar to those of *cis,mer*-Re(CO)$_2$(κ^1-dpm)(κ^2-dpm)Br. The ^{31}P NMR spectrum of the cation is also very similar to that of *cis,mer*-Re(CO)$_2$(κ^1-dpm)(κ^2-dpm)Br, except that the signal due to the pendant phosphorus is no longer present and is replaced by a signal in the region associated with phosphonium salts. Thus, the spectroscopic data indicate that the pendant phosphorus is methylated, and the remainder of the molecule is unchanged.

The IR spectrum of the white solid obtained from the reaction of Re(CO)$_5$Cl and dpe (1:2) in refluxing mesitylene showed two bands in the carbonyl region consistent with a *cis*-dicarbonyl geometry. The ^{31}P NMR spectrum (Figure S6) consists of three signals of equal intensities, all at considerably higher frequency than the resonance of free dpe, indicating that all of the phosphorus atoms are coordinated to the metal. Two of the signals are doublets (J_{P-P} = 180 Hz), which is indicative of trans nonequivalent phosphorus atoms on rhenium. This spectroscopic evidence can be rationalized in terms of a dpe-bridged binuclear complex, but with *cis,mer* geometry rather than the *cis,fac* stereochemistry assigned to the corresponding manganese complex. To confirm the stoichiometry, Re(CO)$_5$X and 1.5 mol of dpe were reacted under the same conditions and the product shows the same ^{31}P NMR spectrum and no resonance for *fac*-Re(CO)$_3$(dpe)X (the known first product of this reaction), indicating that enough dpe is present to react with all the tricarbonyl complex. ESMS data (Table 2), described in more detail later, confirm the empirical formula Re$_2$(CO)$_4$(dpe)$_3$Cl$_2$. Similar observations were made for the corresponding bromo complex. The only structure consistent with all the spectroscopic and mass spectrometric data is *cis,mer*-{Re(CO)$_2$(dpe)X}$_2$(μ-dpe) (structure V), and this is also fully consistent with electrochemical studies described later. A similar complex was synthesized with dpp (dpp = Ph$_2$P(CH$_2$)$_3$PPh$_2$).

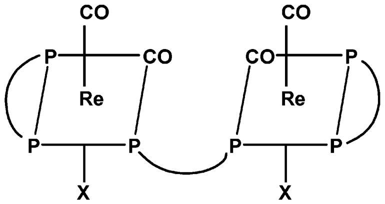

Structure V

Re(CO)$_2$(κ^1-dpe)(κ^2-dpe)X is synthesized by reacting Re(CO)$_5$X in a 1:2 molar ratio with dpe under milder conditions in refluxing xylene. The ^{31}P NMR spectrum consists of four resonances of equal intensities, three of them at positions almost identical with those of *cis,mer*-{Re(CO)$_2$(dpe)X}$_2$(μ-dpe); the fourth is close to the position of the resonance of free dpe, indicating the compounds to be *cis,mer*-Re(CO)$_2$(κ^1-dpe)(κ^2-dpe)X. The compounds Re(CO)$_2$(κ^1-ape)(κ^2-ape)X (ape = Ph$_2$AsCH$_2$CH$_2$PPh$_2$) were prepared by reacting Re(CO)$_5$X with 2 mol of ape in refluxing mesitylene. IR spectroscopy indicates a *cis*-dicarbonyl arrangement, and the ^{31}P NMR spectrum consists of two doublets with a large coupling constant, suggesting nonequivalent *trans* phosphorus atoms. The data are consistent with a *cis,mer* geometry with the κ^1-ape ligand being phosphorus-bonded. Addition of MeI to this compound gives a derivative for which the IR and ^{31}P NMR spectra are almost unaltered and are consistent with the formulation *cis,mer*-[Re(CO)$_2$(κ^1-apeMe)(κ^2-ape)X]I. Confirmation of stoichiometry is provided by ESMS. The interpretation of IR and ^{31}P NMR spectra (Table 4, Figure S7) of Re compounds generated during the course of bulk electrolysis experiments are provided elsewhere in the text.

B. Electrochemical Studies on *cis,mer*-Mn(CO)$_2$(κ^1-dpm)(κ^2-P-P)X (X = Cl, Br) Complexes. (i) Cyclic Voltammetry. The oxidation of *cis,mer*-Mn(CO)$_2$(κ^1-dpm)(κ^2-dpm)X has been reported in detail elsewhere.[15] In view of the similarity of all of the *cis,mer*-Mn(CO)$_2$(κ^1-dpm)(κ^2-P-P)X complexes, only a brief summary of the voltammetry of some of these dicarbonyls needs to be given. Cyclic voltammetric data obtained at a scan rate of 200 mV s^{-1} in dichloromethane (0.1 M Bu$_4$NPF$_6$) at specified temperatures are summarized in Table 5. On the initial cycle of the potential, an oxidative response (process 1) is observed at the potentials indicated in Table 5. An associated reduction response (process 1′) also is seen for most complexes (Table 5). However, the smaller value of the reduction current indicates that process 1 is not reversible in the chemical sense at a scan rate of 200 mV s^{-1}. A second reduction peak (process 2′) also is observed on the first cycle of the potential, while second and subsequent cycles reveal a corresponding oxidation response (process 2). For redox couple 2, the reduction and oxidation peak height are equal, as expected for a chemically reversible process. Scanning to more positive potentials reveals additional oxidation responses, which are irreversible under all conditions studied and will not be discussed further.

The limiting oxidation current for process 1 at a platinum-microdisk electrode (radius 12.5 μm) is similar to that for an equimolar solution of *fac*-Mn(CO)$_3$(κ^2-dpe)Br, which is known to undergo a one-electron oxidation.[16] The charge-transfer process associated with redox couple 1 is therefore assigned to the reaction

$$\textit{cis,mer}\text{-Mn(CO)}_2(\kappa^1\text{-dpm})(\kappa^2\text{-P-P})\text{X} \rightleftharpoons \textit{cis,mer}\text{-[Mn(CO)}_2(\kappa^1\text{-dpm})(\kappa^2\text{-P-P})\text{X]}^+ + e^- \quad (1)$$

in which the Mn(I) compound is oxidized to the isostructural Mn(II) compound. However, *cis,mer*-[Mn(CO)$_2$(κ^1-dpm)(κ^2-P-P)X]$^+$ rapidly converts to the species reduced in process 2′, which on the basis of data contained in ref 15 is the electronically[17] and sterically preferred *trans*-[Mn(CO)$_2$(κ^1-dpm)(κ^2-P-P)X]$^+$. Redox couple 2 may therefore be assumed to be due to the reaction

$$\textit{trans}\text{-Mn(CO)}_2(\kappa^1\text{-dpm})(\kappa^2\text{-dpm})\text{Br} \rightleftharpoons \textit{trans}\text{-[Mn(CO)}_2(\kappa^1\text{-dpm})(\kappa^2\text{-dpm})\text{Br]}^+ + e^- \quad (2)$$

Overall, therefore, the voltammetric behavior is sum-

---

(15) Eklund, J. C.; Bond, A. M.; Colton, R.; Humphrey, D. G.; Mahon, P. J.; Walter, J. N. *Inorg. Chem.* **1999**, *38*, 2005.

(16) Bond, A. M.; Colton, R.; McDonald, M. E. *Inorg. Chem.* **1978**, *17*, 2842.

(17) Mingos, D. M. P. *Organomet. Chem.* **1979**, *179*, C29.

Table 5. Voltammetric Data (Scan Rate 200 mV s^{-1}) at a Glassy-Carbon-Disk Electrode (Radius 0.5 mm) for Manganese Complexes in Dichloromethane (0.1 M Bu_4NPF_6)

compd	process	E_p^{ox} (V)	E_p^{red} (V)	$E_{1/2}$ (V)	ΔE_p (mV)	temp (°C)
cis,mer-$Mn(CO)_2(\kappa^1$-dpm)(κ^2-dpm)Cl	1	0.196	0.106	0.151	90	20
	1	0.204	0.104	0.154	100	−30
	2	−0.344	−0.422	−0.383	78	20
(actually $[Mn(CO)_2(dpm)_2]^{2+/+}$)	3	0.414	0.320	0.367	94	20
cis,mer-$Mn(CO)_2(\kappa^1$-dpm)(κ^2-dpm)Br	1	0.204	0.114	0.159	90	20
	1	0.214	0.112	0.163	102	−30
	2	−0.333	−0.413	−0.373	80	20
(actually $[Mn(CO)_2(dpm)_2]^{2+/+}$)	3	0.428	0.304	0.366	124	20
cis-$Mn(CO)_2(\kappa^1$-dpm)(κ^2-dpe)Br	1	0.208				20
	1	0.228	0.120	0.174	108	−40
	2	−0.285	−0.361	−0.323	76	20
cis-$Mn(CO)_2(\kappa^1$-dpm)(κ^2-dpbz)Br	1	0.210				20
	1	0.232	0.118	0.175	114	−40
	2	−0.233	−0.309	−0.271	76	20
cis,fac-{$Mn(CO)_2$(dpe)Cl}$_2$(μ-dpe)	(1)	0.182				20
	(2)	0.310				20
	1	0.235	0.103	0.169	132	−50
	2	0.365	0.221	0.293	144	−50
	3	−0.321	−0.417	−0.369	96	20
	4	−0.200	−0.290	−0.245	90	20
cis,fac-{$Mn(CO)_2$(dpe)Br}$_2$(μ-dpe)	(1)	0.191				20
	(2)	0.332				20
	1	0.247	0.113	0.180	134	−50
	2	0.390	0.250	0.320	140	−50
	3	−0.278	−0.368	−0.323	90	20
	4	−0.176	−0.262	−0.219	86	20

marized by a limited version of a square scheme:[18]

$$\begin{tikzcd} cis,mer\text{-}Mn(CO)_2(\kappa^1\text{-dpm})(\kappa^2\text{-P-P})X \arrow[r, rightleftharpoons] & cis,mer\text{-}[Mn(CO)_2(\kappa^1\text{-dpm})(\kappa^2\text{-P-P})X]^+ + e^- \arrow[d, "k_1"] \\ trans\text{-}Mn(CO)_2(\kappa^1\text{-dpm})(\kappa^2\text{-P-P})X \arrow[r, rightleftharpoons] & trans\text{-}[Mn(CO)_2(\kappa^1\text{-dpm})(\kappa^2\text{-P-P})X]^+ + e^- \end{tikzcd}$$

(3)

(ii) Bulk Electrolysis. Bulk electrolyses of dichloromethane (0.1 M Bu_4NPF_6) solutions of *cis*-$Mn(CO)_2$(κ^1-dpm)(κ^2-P-P)X were performed initially at −40 °C to prevent chelation of the dpm in the 17e cation.[15] In each case, the amount of charge passed corresponds to a one-electron oxidation process when the potential is held close to E_p^{ox} of process 1. Steady-state voltammograms obtained at a Pt-microdisk electrode during the course of these bulk oxidative experiments show that redox couple 1 is absent after electrolysis, while reversible redox couple 2 is observed as a reduction process. The IR spectra of these solutions (Table 3) each display a single strong carbonyl stretch corresponding to formation of *trans*-$[Mn(CO)_2(\kappa^1$-dpm)(κ^2-P-P)X]$^+$. Bulk reduction (−40 °C) of each solution at a potential slightly more negative than E_p^{red} for process 2 generated the oxidative component of process 2 (shown by steady-state voltammograms) via a one-electron process. The IR spectra of these solutions, acquired quickly at room temperature (Table 3), show a single carbonyl stretch corresponding to *trans*-$Mn(CO)_2(\kappa^1$-dpm)(κ^2-P-P)X. The ^{31}P NMR spectrum (Figure S2) of each reduced solution containing 0.4 M Bu_4NCO_4 as the electrolyte displays four signals of equal intensities (Table 3), which is further evidence that the reductive component of process 2 generates *trans*-$Mn(CO)_2(\kappa^1$-dpm)(κ^2-P-P)X. At room temperature, chelation of the pendant phosphorus in *trans*-$[Mn(CO)_2(\kappa^1$-dpm)(κ^2-P-P)X]$^+$ occurs to give the *trans*-$[Mn(CO)_2(\kappa^2$-dpm)(κ^2-P-P)]$^+$ complex.[16] Thus, the reaction scheme given in eq 3 is verified by bulk electrolysis and spectroscopic characterization of products at low temperatures.

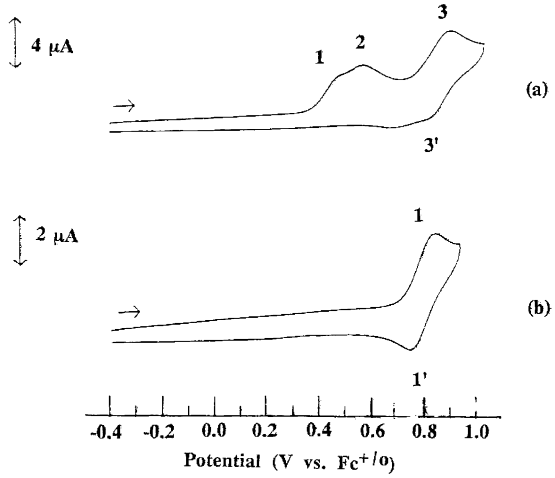

Figure 1. Oxidative cyclic voltammograms at a glassy-carbon electrode (radius 0.5 mm) of 1.0 mM solutions of (a) *cis,mer*-$Re(CO)_2(\kappa^1$-dpm)(κ^2-dpm)Br and (b) *cis,mer*-$Re(CO)_2(\kappa^1$-dpmMe)(κ^2-dpm)Br in dichloromethane (0.1 M Bu_4NPF_6) at 22 °C using a scan rate of 200 mV s^{-1}.

C. Electrochemical Studies on *cis,mer*-$Re(CO)_2$(κ^1-dpm)(κ^2-dpm)X and *cis,mer*-$Re(CO)_2$(κ^1-dpmO)(κ^2-dpm)X. (i) Cyclic Voltammetry. A cyclic voltammogram of a 1.0 mM solution of *cis,mer*-$Re(CO)_2(\kappa^1$-dpm)(κ^2-dpm)Br in dichloromethane (0.1 M Bu_4NPF_6) at 22 °C shows an initial oxidation response occurring at 0.472 V (process 1), which is unresolved from a second response, process 2 (Figure 1a). At more positive potentials a third response (process 3) is observed, and the reductive direction reverse scan reveals some reduction current (process 3′). When the scan direction is switched after either process 1 or 2, no reductionresponse is observed. Since the oxidation of the rhenium center occurs at a considerably more positive potential

---

[18] (a) Bond, A. M.; Colton, R. *Coord. Chem. Rev.* **1997**, *166*, 161. (b) Bond, A. M.; Colton, R.; Jackowski, J. J. *Inorg. Chem.* **1975**, *14*, 274.

than the corresponding process for manganese, it was considered possible that the first irreversible oxidation response (process 1) might be associated with oxidation of the pendant phosphorus atom to an oxide. This was confirmed by examining the cyclic voltammetry of an authentic sample of *cis,mer*-Re(CO)$_2$(κ^1-dpmO)(κ^2-dpm)-Br, which gives processes 2 and 3 but not process 1. Process 1 is therefore assigned to the overall reaction

$$\textit{cis,mer}\text{-Re(CO)}_2(\kappa^1\text{-dpm})(\kappa^2\text{-dpm})\text{Br} + \text{H}_2\text{O} \rightarrow \textit{cis,mer}\text{-Re(CO)}_2(\kappa^1\text{-dpmO})(\kappa^2\text{-dpm})\text{Br} + 2\text{H}^+ + 2\text{e}^- \quad (4)$$

assuming that the reaction involves the initial formation of a phosphonium cation radical and subsequent reaction with traces of water in the system. This reaction in eq 4 could not be prevented even when using dichloromethane dried for extended periods of time over molecular sieves or alumina. Process 2 may then be assigned to the chemically irreversible oxidation of *cis,mer*-Re(CO)$_2$(κ^1-dpmO)(κ^2-dpm)Br. Similar observations were made with *cis,mer*-Re(CO)$_2$(κ^1-dpm)(κ^2-dpm)Cl and *cis,mer*-Re(CO)$_2$(κ^1-dpmO)(κ^2-dpm)Cl. Further evidence for the assignment of processes 1 and 2 and a discussion of process 3 will be given below, after consideration of data obtained by bulk oxidative electrolysis.

(ii) Bulk Electrolysis. Due to the similar potentials of processes 1 and 2, which prevented selective oxidation, a solution of *cis,mer*-Re(CO)$_2$(κ^1-dpm)(κ^2-dpm)Br in dichloromethane (0.4 M Bu$_4$NClO$_4$) was partially oxidized at a potential corresponding to the foot of process 1, and the solution was monitored by ^{31}P NMR spectroscopy. The spectra acquired at various stages of the electrolysis show the growth of signals due to *cis,mer*-Re(CO)$_2$(κ^1-dpmO)(κ^2-dpm)Br (Table 2). When the potential is made more positive, these signals in the NMR spectrum broaden and numerous other resonances are observed. New voltammetric responses are observed temporarily during this stage of the electrolysis, but process 3, which is reversible, is the only permanent response, as long as the applied electrolysis potential is kept less positive than that of process 3. The ^{31}P NMR spectrum of the fully electrolyzed solution (Figure S7), which shows only redox couple 3, has two resonances of equal intensities. The IR spectrum shows two carbonyl bands consistent with a *cis*-dicarbonyl geometry. Exhaustive bulk electrolysis of a fresh solution of *cis,mer*-Re(CO)$_2$(κ^1-dpm)(κ^2-dpm)Br shows that the overall reaction to produce redox couple 3 is an overall apparently six-electron process.

In the case of bulk oxidative electrolysis of *cis,mer*-Re(CO)$_2$(κ^1-dpm)(κ^2-dpm)Cl, the final IR and ^{31}P NMR spectra are very similar to those derived from *cis,mer*-Re(CO)$_2$(κ^1-dpm)(κ^2-dpm)Br. However, the exhaustive electrolysis experiment shows that five rather than six electrons are apparently involved in the complete oxidation in this case. Bulk electrolysis of *cis,mer*-Re(CO)$_2$(κ^1-dpmO)(κ^2-dpm)Br also gave the same final product associated with process 3 via an overall four-electron process, while *cis,mer*-Re(CO)$_2$(κ^1-dpmO)(κ^2-dpm)Cl is exhaustively oxidized to also give the same product in an overall three-electron process.

ESMS experiments and spectroscopic data (described later) show that the ion [Re(CO)$_2$(dpmO)$_2$]$^+$ is present in the exhaustively electrolyzed solutions, and redox couple 3 is assigned to the reaction

$$[\text{Re(CO)}_2(\text{dpmO})_2]^+ \rightleftharpoons [\text{Re(CO)}_2(\text{dpmO})_2]^{2+} + \text{e}^- \quad (5)$$

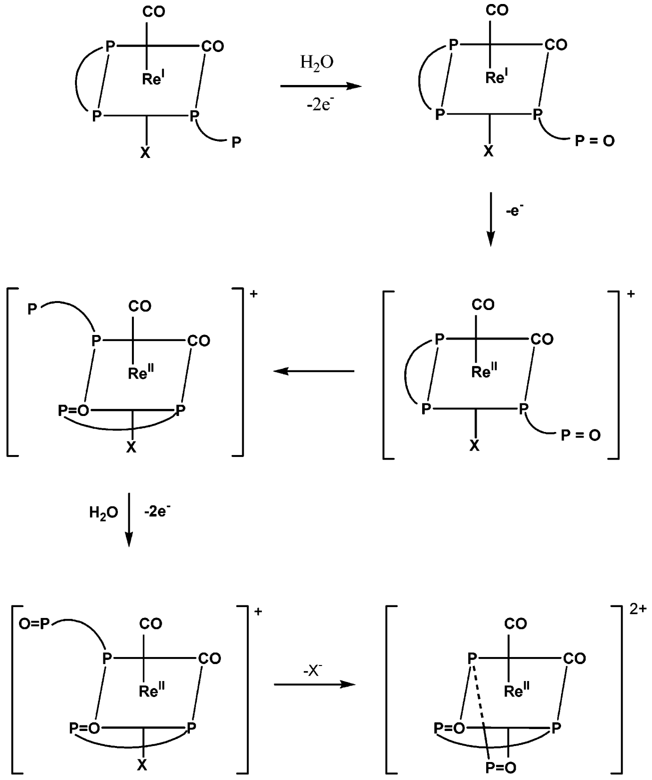

Figure 2. Proposed mechanism for the formation of *cis*-[Re(CO)$_2$(dpmO)$_2$]$^+$.

The mechanism proposed for the oxidation of *cis,mer*-Re(CO)$_2$(κ^1-dpm)(κ^2-dpm)Br is shown in Figure 2. Two electrons are required to oxidize each of the two P(III) atoms to P(V), one to oxidize Re(I) to Re(II) and one to oxidize bromide to bromine. The final product of this scheme is [Re(CO)$_2$(dpmO)$_2$]$^{2+}$, but at the potential applied to the electrode (less positive than process 3) it will be reduced to [Re(CO)$_2$(dpmO)$_2$]$^+$. The charge passed in the reverse direction is not subtracted by the instrument used; thus, an apparently six-electron reaction is indicated. However, the overall reaction is actually a five-electron oxidation process:

$$\textit{cis,mer}\text{-Re(CO)}_2(\kappa^1\text{-dpm})(\kappa^2\text{-dpm})\text{Br} + 2\text{H}_2\text{O} \rightarrow \textit{cis}\text{-[Re(CO)}_2(\text{dpmO})_2]^+ + {}^1/_2\text{Br}_2 + 4\text{H}^+ + 5\text{e}^- \quad (6)$$

In the case of the chloro compound, the overall reaction is very similar but the applied potential is not sufficiently positive to oxidize the displaced chloride ion to chlorine, thus leading to

$$\textit{cis,mer}\text{-Re(CO)}_2(\kappa^1\text{-dpm})(\kappa^2\text{-dpm})\text{Cl} + 2\text{H}_2\text{O} \rightarrow \textit{cis}\text{-[Re(CO)}_2(\text{dpmO})_2]^+ + \text{Cl}^- + 4\text{H}^+ + 4\text{e}^- \quad (7)$$

Another minor side reaction must occur in this case, as the coulometric count approaches five rather than four electrons. Obviously, as observed, the electron count is expected to be less when the electrolysis commences with the partially oxidized species *cis,mer*-Re(CO)$_2$(κ^1-dpmO)(κ^2-dpm)X, rather than *cis,mer*-Re(CO)$_2$(κ^1-dpm)(κ^2-dpm)X.

The two structures VIa and VIb for *cis*-[Re(CO)$_2$(dpmO)$_2$]$^+$ are both consistent with the ^{31}P NMR and IR spectra, but ^{13}C NMR spectroscopy should distinguish between them, since a carbonyl trans to oxygen should give a singlet resonance, while one trans to phosphorus should be a doublet. The ^{13}C NMR spectrum (carbonyl region) of *cis*-[Re(CO)$_2$(dpmO)$_2$]$^+$ is a singlet; therefore, structure VIa is indicated.

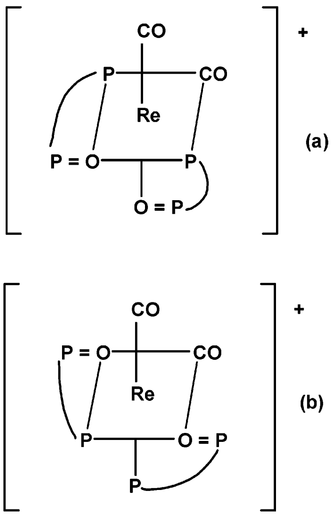

Structure VI

D. Voltammetric Studies on *cis,mer*-[Re(CO)$_2$(κ^1-dpmMe)(κ^2-dpm)X]PF$_6$. If the mechanism for oxidation of *cis,mer*-Re(CO)$_2$(κ^1-dpm)(κ^2-dpm)X is correct, then methylation of the pendant phosphorus in *cis,mer*-Re(CO)$_2$(κ^1-dpm)(κ^2-dpm)X to give *cis,mer*-[Re(CO)$_2$(κ^1-dpmMe)(κ^2-dpm)Br]PF$_6$ should remove the phosphorus oxidation reaction in the electrochemical studies. An oxidative cyclic voltammogram of a 1.0 mM solution of *cis,mer*-[Re(CO)$_2$(κ^1-dpmMe)(κ^2-dpm)Br]PF$_6$ in dichloromethane (0.1 M Bu$_4$NPF$_6$) shows an oxidative response at 0.836 V (process 1), and on the reverse scan, the corresponding reduction response (process 1′) is observed (Figure 1b). Analysis of the steady-state voltammogram at a platinum microelectrode indicates that this is a one-electron process and is assigned to the reaction

$$\textit{cis,mer}\text{-}[\mathrm{Re(CO)_2}(\kappa^1\text{-dpmMe})(\kappa^2\text{-dpm})\mathrm{Br}]^+ \rightleftharpoons \textit{cis,mer}\text{-}[\mathrm{Re(CO)_2}(\kappa^1\text{-dpmMe})(\kappa^2\text{-dpm})\mathrm{Br}]^{2+} + e^- \quad (8)$$

where Re(I) is oxidized to Re(II). The chloro complex exhibits similar voltammetry, although it is interesting that there is no evidence for isomerization to the *trans* isomer on the voltammetric time scale.

E. Electrochemical Studies on *cis,mer*-[Re(CO)$_2$(κ^1-ape)(κ^2-ape)X. (i) Cyclic Voltammetry. An oxidative cyclic voltammogram of a 1.0 mM solution of *cis,mer*-Re(CO)$_2$(κ^1-ape)(κ^2-ape)Cl in dichloromethane (0.1 M Bu$_4$NPF$_6$) at 20 °C and with a scan rate of 200 mV s^{-1} shows a partially reversible process 1 at 0.578 V and a second smaller reversible process 2 at 0.726 V. On second and successive scans, process 1 diminishes while process 2 becomes dominant. Lowering the temperature leads to enhanced reversibility in the first process, a decrease in the current for process 2 relative to that for process 1, until this more positive process is barely detected at −70 °C. The charge-transfer step associated with process 1 is assigned to the couple

$$\textit{cis,mer}\text{-}\mathrm{Re(CO)_2}(\kappa^1\text{-ape})(\kappa^2\text{-ape})\mathrm{Cl} \rightleftharpoons \textit{cis,mer}\text{-}[\mathrm{Re(CO)_2}(\kappa^1\text{-ape})(\kappa^2\text{-ape})\mathrm{Cl}]^+ + e^- \quad (9)$$

The temperature dependence of the voltammetric data suggest that process 2 is associated with oxidation of a species formed from a chemical step following the charge-transfer process, the rate of which is slowed upon cooling the solution. Similar observations were made for the bromo complex, and data are summarized in Table 6.

(ii) Bulk Electrolysis. Exhaustive bulk electrolysis of a dichloromethane solution (0.4 M Bu$_4$NClO$_4$) of *cis,mer*-Re(CO)$_2$(κ^1-ape)(κ^2-ape)Br was carried out at a potential slightly less than E_p^ox of process 1. A cyclic voltammogram of the resulting solution shows process 1 to be absent with process 2 present. However, a steady-state voltammogram indicates that process 2 is present as a reduction rather than an oxidation reaction.

Both the IR and ^{31}P NMR spectra of this solution are similar to those of the starting material (Table 4), suggesting that the overall reaction may only involve change at the pendant arsenic atom. ESMS (see later) gives a clear indication that the cation *cis,mer*-[Re(CO)$_2$(κ^1-apeO)(κ^2-ape)Br]$^+$ is present in the solution; therefore, process 2 is assigned to the redox couple

$$\textit{cis,mer}\text{-}[\mathrm{Re(CO)_2}(\kappa^1\text{-apeO})(\kappa^2\text{-ape})\mathrm{Br}]^+ \rightleftharpoons \textit{cis,mer}\text{-}[\mathrm{Re(CO)_2}(\kappa^1\text{-apeO})(\kappa^2\text{-ape})\mathrm{Br}]^{2+} + e^- \quad (10)$$

The product is in the reduced form because the applied potential is less positive than the reversible potential for process 2. The exact mechanism for the formation of the κ^1-apeO complex is not known, but it clearly involves some reaction of the initially produced *cis,mer*-[Re(CO)$_2$(κ^1-ape)(κ^2-ape)Br]$^+$, presumably with traces of water in the system, to give an equation analogous to that given for the oxidation of the *cis,mer*-[Re(CO)$_2$(κ^1-dpm)(κ^2-dpm)Br] reaction (see eq 4).

F. Electrochemical Studies of *cis,mer*-[Re(CO)$_2$(κ^1-apeMe)(κ^2-ape)X]$^+$. An oxidative cyclic voltammogram of a 1.0 mM solution of *cis,mer*-[Re(CO)$_2$(κ^1-apeMe)(κ^2-ape)Br]$^+$ in dichloromethane (0.1 M Bu$_4$PF$_6$) shows the presence of only a single reversible process 1. Analysis of a steady-state voltammogram indicates that this is a reversible one-electron process, which is therefore assigned to the redox couple

$$\textit{cis,mer}\text{-}[\mathrm{Re(CO)_2}(\kappa^1\text{-apeMe})(\kappa^2\text{-ape})\mathrm{Br}]^+ \rightleftharpoons \textit{cis,mer}\text{-}[\mathrm{Re(CO)_2}(\kappa^1\text{-apeMe})(\kappa^2\text{-ape})\mathrm{Br}]^{2+} + e^- \quad (11)$$

Since the pendant arsenic atom cannot be oxidized in this compound, the absence of a second process is consistent with the identification of process 2 made above.

G. Electrochemical Studies on *cis,fac*-{Mn(CO)$_2$(dpe)X}$_2$(μ-dpe) (X = Cl, Br). (i) Cyclic Voltammetry. The cyclic voltammetry of the binuclear species is

Table 6. Voltammetric Data (20 °C, Scan Rate 200 mV s^{-1}) at a Glassy-Carbon-Disk Electrode (Radius 0.5 mm) for Rhenium Complexes in Dichloromethane (0.1 M Bu_4NPF_6)

initial compd	process	E_p^{ox} (V)	E_p^{red} (V)	$E_{1/2}$ (mV)	ΔE_p
cis,mer-$Re(CO)_2(\kappa^1\text{-dpm})(\kappa^2\text{-dpm})Cl$	1	0.525[a]			
	2	0.525[a]			
	3	0.875	0.783	0.829	92
cis,mer-$[Re(CO)_2(\kappa^1\text{-dpmMe})(\kappa^2\text{-dpm})Cl]PF_6$	1	0.837	0.749	0.793	88
cis,mer-$Re(CO)_2(\kappa^1\text{-dpm})(\kappa^2\text{-dpm})Br$	1	0.472			
	2	0.549			
	3	0.898	0.808	0.853	90
cis,mer-$[Re(CO)_2(\kappa^1\text{-dpmMe})(\kappa^2\text{-dpm})Br]PF_6$	1	0.836	0.746	0.791	90
cis,mer-$\{Re(CO)_2(dpe)Cl\}_2(\mu\text{-dpe})$	1	0.492	0.406	0.449	86
	2	0.634	0.540	0.587	94
	3	1.028			
cis,mer-$\{Re(CO)_2(dpe)Br\}_2(\mu\text{-dpe})$	1	0.496	0.408	0.452	88
	2	0.640	0.548	0.594	92
	3	1.020			
cis,mer-$\{Re(CO)_2(dpp)Br\}_2(\mu\text{-dpp})$	1	0.500	0.410	0.455	90
	2	0.608	0.512	0.560	96
	3	0.956			
cis,mer-$Re(CO)_2(\kappa^1\text{-ape})(\kappa^2\text{-ape})Cl$	1	0.578	0.488	0.533	90
	2	0.726	0.638	0.682	88
cis,mer-$[Re(CO)_2(\kappa^1\text{-apeMe})(\kappa^2\text{-ape})Cl]PF_6$	1	0.724	0.630	0.677	94
cis,mer-$Re(CO)_2(\kappa^1\text{-ape})(\kappa^2\text{-ape})Br$	1	0.608	0.514	0.561	94
	2	0.740	0.648	0.694	92
cis,mer-$[Re(CO)_2(\kappa^1\text{-apeMe})(\kappa^2\text{-ape})Br]PF_6$	1	0.720	0.630	0.675	90

[a] The potentials of these processes overlap.

extremely complicated. There are always both oxidation and reduction components, and the nature of the voltammetry is critically dependent upon temperature. Since detailed assignments cannot be made until the spectroscopic characteristics of the system have been determined after bulk electrolysis experiments (see later), these initial voltammetric section responses will be indicated as, for example, process (1) (indicating complexity within process 1) and detailed mechanistic discussion will be given later. Voltammetric data are summarized in Table 5.

Oxidative cyclic voltammograms at a glassy-carbon-disk electrode (radius 0.5 mm) for a 1.0 mM solution of *cis,fac*-$\{Mn(CO)_2(dpe)Br\}_2(\mu\text{-dpe})$ in dichloromethane (0.1 M Bu_4NPF_6) are shown in Figure 3. The first scan of the voltammogram at 20 °C (Figure 3a) displays oxidation responses at 0.191 V (process (1)) and 0.332 V (process (2)), which are irreversible when the scan is reversed after process (2). However, the reduction waves are observed at more negative potentials (processes (3′) and (4′)) and a second scan reveals the oxidative components of the reversible redox couples (3) and (4). Figure 3b shows an oxidative cyclic voltammogram in which the potential is reversed immediately after process (1). The reverse scan shows only the reduction process (3′), and the related oxidation response, process (3), is seen on the second scan. A steady-state voltammogram at a platinum-microdisk electrode (radius 12.5 μm) at 20 °C for the two irreversible oxidation processes (1) and (2) shows that their limiting currents are similar to each other and also similar to the current observed for the first one-electron oxidation of *mer*-$\{Cr(CO)_3(dpe)\}_2(\mu\text{-dpe})$.[19] Thus, it is concluded that processes (1) and (2) each involve one electron on the voltammetric time scale.

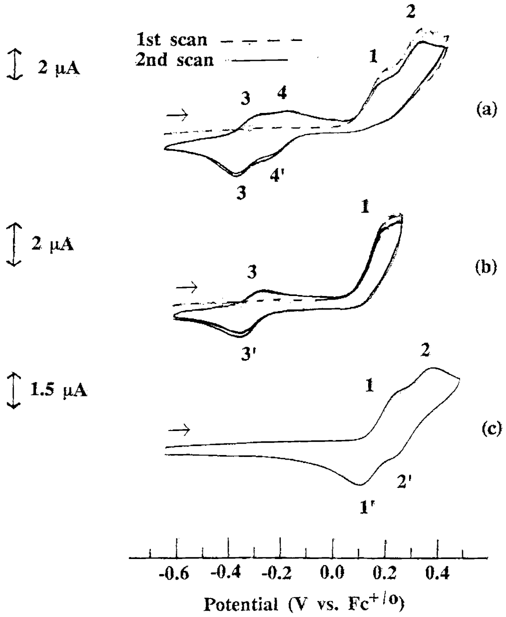

Figure 3. Oxidative cyclic voltammograms at a glassy-carbon electrode (radius 0.5 mm) of a 1.0 mM solution of *cis,fac*-$\{Mn(CO)_2(dpe)Br\}_2(\mu\text{-dpe})$ in dichloromethane (0.1 M Bu_4NPF_6; scan rate 200 mV s^{-1}): (a) at 20 °C; (b) at 20 °C, reversing scan after process 1; (c) at −50 °C.

A cyclic voltammogram of this solution at −50 °C is shown in Figure 3c. Processes (1) and (2) are now chemically reversible, and reduction processes (3′) and (4′) are no longer observed. This indicates that the species giving rise to redox couples (3) and (4) result from chemical steps after oxidation processes (1) and (2). The evidence presented earlier shows that redox couple (3) is associated with a product formed from chemically irreversible process (1) and redox couple (4) is associated with chemically irreversible process (2). In view of the common experience of isomerization following oxidation,[18] it is suggested that isomerization of one metal center occurs after process (1) to give a mixed-geometry binuclear complex (*cis,fac*^{0}/*trans*$^+$) and, following process (2), both metal centers become *trans* ($\{trans^+\}_2$), and it is these species which give rise to

---

(19) Bond, A. M.; Colton, R.; Cooper, J. B.; McGregor, K.; Walter, J. N.; Way, D. M. *Organometallics* **1995**, *14*, 49.

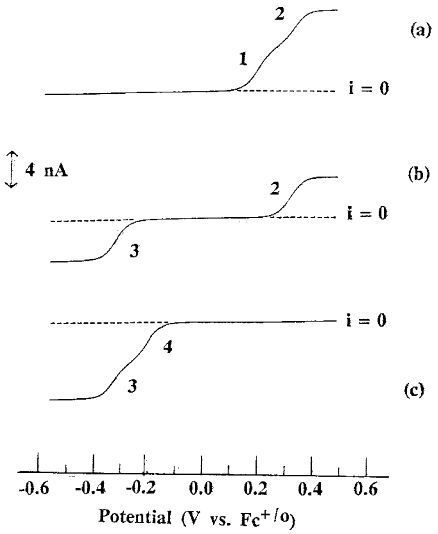

Figure 4. Steady-state voltammograms at a platinum microelectrode (radius 12.5 μm) of a 1.0 mM solution of *cis*,-*fac*-{Mn(CO)$_2$(dpe)Br}$_2$(μ-dpe) in dichloromethane (0.1 M Bu$_4$NPF$_6$) at different stages during bulk electrolysis at 20 °C: (a) before electrolysis; (b) after exhaustive oxidative electrolysis at a potential slightly less positive than E_p^{ox} for process 1; (c) after exhaustive oxidative electrolysis at a potential slightly more positive than E_p^{ox} for process 2.

redox couples (3) and (4). Support for the validity of these assignments will be given in the next section.

(ii) Bulk Electrolysis. Exhaustive bulk electrolysis at 20 °C of a solution of *cis,fac*-{Mn(CO)$_2$(dpe)Br}$_2$(μ-dpe) in dichloromethane (0.1 M Bu$_4$NPF$_6$) was undertaken at a platinum-gauze working electrode at a potential slightly less positive than E_p^{ox} for process (1). The amount of charge passed after this exhaustive electrolysis corresponds to a one-electron-oxidation process. A steady-state voltammogram of the solution before electrolysis is shown in Figure 4a, and a voltammogram after electrolysis is shown in Figure 4b. Process (1) is absent after a one-electron electrolysis, and the sign of the current indicates that it has been replaced by the reductive component of process (2). Process (3) remains and still involves the same number of electrons in the charge-transfer process as did process (1) before electrolysis. The IR spectrum of the oxidized solution shows three carbonyl stretches. Two at 1937 and 1865 cm^{-1} are identical with those of the starting material and are assigned to the carbonyl groups coordinated to the unoxidized manganese atom in the binuclear complex. The third stretch at 1965 cm^{-1} occurs at a position very close to that observed for *trans*-[Mn(CO)$_2$(κ^1-dpm)(κ^2-dpm)Br]$^{2+}$ and is assigned to *trans* carbonyl groups on the oxidized manganese atom. This stable product of the one-electron oxidation of *cis,fac*-{Mn(CO)$_2$(dpe)Br}$_2$(μ-dpe) is identified as *cis,fac*-Mn(CO)$_2$(dpe)Br(μ-dpe)-*trans*-[Mn(CO)$_2$(dpe)Br]$^+$, simplified to *cis,fac(trans)*-[{Mn(CO)$_2$(dpe)Br}$_2$(μ-dpe)]$^+$.

Further bulk electrolysis of this solution, at a potential slightly more positive than E_p^{ox} for process (2), gives a second one-electron oxidation on the basis of the charge passed. Cyclic voltammograms show that process (2) has been replaced by process (4). A steady-state voltammogram of the oxidized solution (Figure 4c) reveals that the oxidative components of processes (3) and (4) are present in the solution. The IR spectrum shows a single carbonyl stretch at 1965 cm^{-1}, indicating that trans carbonyl groups now are present on both metal centers, and the compound is identified as *trans*-[{Mn(CO)$_2$(dpe)Br}$_2$(μ-dpe)]$^{2+}$.

Exhaustive bulk electrolysis at 20 °C of a fresh dichloromethane solution of *cis,fac*-{Mn(CO)$_2$(dpe)Br}$_2$-(μ-dpe), at a potential slightly more positive than E_p^{ox} for process (2), indicates that two electrons are passed per molecule of compound, and the same final IR spectrum is observed; therefore, the same result is obtained whether the electrolysis is performed in either a one- or two-stage manner.

When a bulk reduction of the fully oxidized solution is carried out at 20 °C at a potential slightly more negative than E_p^{red} for process (3), the amount of charge passed indicates that this is a two-electron process. A steady-state voltammogram shows that processes (3) and (4) are absent after the reduction, but processes (1) and (2) are observed. The current associated with processes (1) and (2) is equal to that for processes (3) and (4) before the reduction, and the voltammogram shows the reductive components of processes (1) and (2) are present in the solution. This result shows that, on the longer time scale of coulometry, the *trans* geometry on the reduced manganese atoms reverts back to the original *cis,mer* geometry.

This isomerization is prevented if the bulk reduction experiment is carried out at −40 °C (after the two-electron oxidation at 20 °C), since under these conditions the steady-state voltammogram shows the reductive components of processes (3) and (4). The IR spectrum of this solution, acquired quickly at room temperature, shows a single band at 1897 cm^{-1}, which is close to the position of the carbonyl stretch for *trans*-Mn(CO)$_2$(κ^1-dpm)(κ^2-dpm)Br (Table 3). The ^{31}P NMR spectrum acquired at −60 °C (Table 3, Figure S4), obtained under the same conditions but with 0.4 M Bu$_4$NClO$_4$ as the electrolyte, displays three signals of equal intensities, all of which occur at higher frequency than the resonance position of free dpe, indicating that all the phosphorus atoms are coordinated to the metal centers. Thus, the spectroscopic data confirm the presence of *trans*-{Mn(CO)$_2$(dpe)Br}$_2$(μ-dpe) in solution after the oxidation and reduction cycle at −40 °C. Similar results are obtained for the corresponding chloro compound.

(iii) Detailed Discussion of the Electrode Processes Detected under Different Conditions. The exact nature of the voltammetric responses observed depends on the conditions, especially the temperature, which determines the rate of isomerization of *cis,fac*$^+$ to *trans*$^+$. Consequently, the voltammetry will be discussed at different temperatures using a shorthand notation which indicates the geometry and charge of the Mn(CO)$_2$(dpe)Br moieties at each end of the dpe bridging ligand.

At −50 °C, the voltammetric oxidation of $(cis,fac^0)_2$ (Figure 3c) exhibits two chemically reversible couples: These are the true couples 1 and 2. However, at 20 °C, the isomerization of *cis,fac*$^+$ to *trans*$^+$ is fast on the voltammetric time scale (Figure 3a); thus, the observed

$$(cis,fac^0)_2 \rightleftharpoons (cis,fac^0)(cis,fac^+) + e^- \text{ (couple 1)} \quad (12)$$

$$(cis,fac^0)(cis,fac^+) \rightleftharpoons (cis,fac^+)_2 + e^- \text{ (couple 2)} \quad (13)$$

responses (1) and (2) are actually due to

$$(cis,fac^0)_2 \rightleftharpoons (cis,fac^0)(cis,fac^+) + e^- \xrightarrow{\text{fast}} (cis,fac^0)(trans^+) \text{ (process (1))} \quad (14)$$

$$(cis,fac^0)(trans^+) \rightleftharpoons (cis,fac^+)(trans^+) + e^- \xrightarrow{\text{fast}} (trans^+)_2 \text{ (process (2))} \quad (15)$$

Thus, on the reverse scan, the reduction processes in Figure 3a are

$$(trans^+)_2 + e^- \rightleftharpoons (trans^0)(trans^+) \text{ (couple 4)} \quad (16)$$

$$(trans^0)(trans^+) + e^- \rightleftharpoons (trans^0)_2 \text{ (couple 3)} \quad (17)$$

and these are the true redox couples 3 and 4, because isomerization of *trans* bulk to the starting material cis,fac^0 is slow on the voltammetric time scale. Alternatively, these couples 3 and 4 also may be observed after exhaustive oxidative electrolysis of $(cis,fac^0)_2$ at a potential corresponding to process (2), which also generates $(trans^+)_2$.

The processes shown in Figure 3b are subtly different. When only the initial one electron oxidation is carried out at room temperature, the product is $(cis,fac^0)(trans^+)$ and its reduction to $(cis,fac^0)(trans^0)$ appears as process (3′). Since isomerization of $trans^0$ to cis,fac^0 is slow on the voltammetic time scale, the oxidation response (3) is due to the reoxidation of $(cis,fac^0)(trans^0)$ to $(cis,fac^0)(trans^+)$ which occurs at a potential close to that of couple 3 (eq 17). Couple 4 is the simplest response of all and is given only by the process shown in eq 16.

The fact that the reversible potentials for the four couples (eqs 12, 13, 15, and 16) and other electron-transfer reactions involving $(cis,fac^0)(trans^+)$ differ implies that a large number of thermodynamically favored second-order cross-redox reactions can occur, e.g.

$$(trans^+)_2 + (cis,fac^0)_2 \rightarrow (trans^+,trans^0) + (cis,fac^+)$$

These reaction pathways can give rise to a range of homogeneous reactions that are may be coupled to the electron-transfer processes and hence modify (catalyze) isomerization reactions. These second-order processes have not been included in the above discussion of the voltammetry, bulk electrolysis, or isomerization processes.

The potentials of processes (1)−(4) are determined predominantly by the ligand geometry of the metal atom being oxidized/reduced (processes (1) and (2) for *cis,fac* and processes (3) and 4 for *trans*) and the charges involved in the process (+/0 and 2+/+). The potential difference between $cis,fac^{+/0}$ and $trans^{+/0}$ (couples 1 and 3) is exactly the same (538 mV) as between $cis,fac^{2+/+}$ and $trans^{2+/+}$ (couples 2 and 4), and is similar to values observed in other systems.[18] The difference in potential for successive oxidations for each geometry (couples 1 and 2 for *cis,fac* and couples 3 and 4 for trans) are also equal at 124 mV, and again this value is typical for successive oxidations in binuclear species of this kind.[19] This relatively small difference in potential between isostructural redox couples implies that the two redox centers are not strongly interacting. This is consistent with the earlier discussion of the IR changes that takes place upon oxidation, which led to the conclusion that significant charge delocalization does not appear to be evident in the mixed valent $(cis,fac^0)(trans^+)$ complexes. The potential changes introduced by chemical irreversibility (processes (1) and (2) at 20 °C) and variation of the geometry of the moiety at the other end of the bridge (couple 3 and process (3)) appear to be relatively small.

H. Electrochemical Studies of *cis,mer*-$\{Re(CO)_2(dpe)X\}_2(\mu\text{-dpe})$. An oxidative cyclic voltammogram of a 1.0 mM solution of *cis,mer*-$\{Re(CO)_2(dpe)Br\}_2(\mu\text{-dpe})$ in dichloromethane (0.1 M Bu_4NPF_6) shows two reversible couples 1 and 2 for all cycles of the potential at a scan rate of 200 mV s^{-1}, and there is no indication on this time scale of any isomerization to the trans geometry. A steady-state voltammogram indicates that each process involves one electron, and these waves are assigned to the consecutive oxidations of the two rhenium atoms from Re(I) to Re(II)

$$cis,mer\text{-}\{Re(CO)_2(dpe)Br\}_2(\mu\text{-dpe}) \rightleftharpoons cis,mer\text{-}[\{Re(CO)_2(dpe)Br\}_2(\mu\text{-dpe})]^+ + e^- \quad (18)$$

$$cis,mer\text{-}[\{Re(CO)_2(dpe)Br\}_2(\mu\text{-dpe})]^+ \rightleftharpoons cis,mer\text{-}[\{Re(CO)_2(dpe)Br\}_2(\mu\text{-dpe})]^{2+} + e^- \quad (19)$$

At more positive potentials, an irreversible oxidation response (process 3) is observed, which probably involves further oxidation of the metal centers. Similar responses are observed for *cis,mer*-$\{Re(CO)_2(dpp)Br\}_2(\mu\text{-dpp})$, and data for all compounds of this type are summarized in Table 6.

I. Electrospray Mass Spectrometry. (i) Manganese Complexes. ESMS provides an independent probe to verify the stoichiometry, but not the isomeric form, of species in solution and is used in this paper to provide additional verification of the identity of the compounds generated electrochemically. For ionic compounds, the cation may be observed directly without problems, but also there are now a number of recognized techniques to convert unobservable neutral species into predictable and closely related ionic derivatives which may be observed by ESMS.[20] For example, neutral species such as metal Schiff base complexes, ML_2, may be protonated by the mobile phase in the spectrometer (frequently H_2O/MeOH/HOAc 50:50:1) and the intact ions $[HML_2]^+$ are readily observed.[21] Alternatively, metal ion addition (metal adduction) may sometimes be successful; for example, in the presence of sodium ions in the solution the neutral anticancer agent *cis*-$PtCl_2(NH_3)_2$ gives the ion $[Na + PtCl_2(NH_3)_2]^+$.[22] Such methods also are frequently applicable with respect to carbonyl complexes.

All ESMS data for manganese complexes are summarized in Table 1. Addition of sodium ions to a solution of *fac*-$Mn(CO)_3(dpe)Br$ enables observation of the ion $[Na + Mn(CO)_3(dpe)Br]^+$ (*m/z* 641). Another peak at *m/z* 537 is assigned to the ion $[Mn(CO)_3(dpe)]^+$ and is formed by elimination of NaBr. Increasing the B1 voltage

---

[20] Colton, R.; D'Agostino, A.; Traeger, J. C. *Mass Spectrom. Rev.* **1995**, *14*, 79.

[21] Cardwell, T. J.; Colton, R.; Mitchell, S.; Traeger, J. C. *Inorg. Chim. Acta* **1994**, *216*, 75.

[22] Poon, G. K.; Mistry, P.; Lewis, S. *Biol. Mass Spectrom.* **1991**, *20*, 687.

causes this peak to increase in relative intensity, thereby demonstrating that it is formed from the intact ion by collisional activation in the gas phase. Similarly, addition of sodium ions to *cis,mer*-Mn(CO)$_2$(κ^1-dpm)(κ^2-dpm)Br gives the sodium adduct of the intact molecule [Na + Mn(CO)$_2$(dpm)$_2$Br]$^+$ (*m/z* 983), together with a number of other ions, including [Mn(CO)$_2$(dpm)$_2$]$^+$ (loss of NaBr) and [Mn(CO)$_2$(dpmO)(dpm)]$^+$ (*m/z* 895). Oxidation of phosphine ligands, especially those with pendant phosphorus atoms, is a common observation in ESMS.[24] A number of the Mn(CO)$_2$(κ^1-dpm)(κ^2-P-P)X compounds were examined by ESMS without any additives in the solution, and in all cases the ions [H + Mn(CO)$_2$(dpm)(P-P)X]$^+$ are observed (Table 1). These are probably simple protonated species, with the proton being derived from the mobile phase. It is important to realize that observation of such protonated species does not imply that a considerable fraction of the solute is protonated; indeed all the indications are that these manganese carbonyl derivatives are not very basic. However, the combination of the extreme sensitivity of mass spectrometry and the inability of the technique to detect the neutral unprotonated molecules allow the observation of minute proportions of protonated species. These in turn allow confirmation of the stoichiometry of the compound in solution.

The oxidant NOBF$_4$ was added to the solutions of the binuclear molecules *cis,fac*-{Mn(CO)$_2$(dpe)X}$_2$(μ-dpe) to generate the cationic forms which then are observed, thus confirming unequivocally the binuclear nature of the compounds.

(ii) Rhenium Complexes. All ESMS data for rhenium complexes are summarized in Table 2. Ionic species such as *cis,mer*-[Re(CO)$_2$(κ^1-dpmMe)(κ^2-dpm)X]PF$_6$ and *cis*-[Re(CO)$_2$(dpmO)$_2$]ClO$_4$ all give a strong peak for their intact cations. Neutral monomeric species such as *cis,mer*-[Re(CO)$_2$(κ^1-dpm)(κ^2-dpm)Br are observed as either their sodium ion adducts or as protonated species. ESMS provides unequivocal proof for the binuclear nature of the species, formulated as *cis,mer*-{Re(CO)$_2$(dpe)X}$_2$(μ-dpe), since they were observed as both their intact sodium adducts and as the intact corresponding singly charged cation after addition of the one-electron chemical oxidant NOBF$_4$.

General Discussion and Conclusions

The chemistry of the diphosphine derivatives of the group 7 carbonyl halides is very rich in both the 18e and 17e oxidized states. In the 18e M(I) complexes, the main variations detected in the chemistry are a function of the ligands; dpm easily forms κ^1/κ^2 derivatives, while dpe clearly shows a preference to coordinate both its phosphorus atoms, either as in the μ-dpe dimers or, under more forcing conditions, the κ^2 complexes *cis*-[Re(CO)$_2$(dpe)$_2$]$^+$ and *trans*-Re(CO)(dpe)$_2$X.

The chemistry of the 17e M(II) species formed by electrochemical oxidation is even more varied and shows considerable differences between the chemistries of the two metals. It is well established[18] that the oxidation potentials of complexes of the second-/third-row metals are more positive than those of the corresponding first-row metal derivatives. This has interesting consequences in the case of the M(CO)$_2$(κ^1-dpm)(κ^2-dpm)X complexes, as the oxidation potential for the pendant phosphine lies between the oxidation potentials for the two metals. The manganese compounds are well-behaved in the sense that the metal-based oxidation is accompanied by the usual isomerization to a *trans*-carbonyl arrangement, but there is the added feature of slow displacement of the halo ligand to generate [Mn(CO)$_2$(dpm)$_2$]$^{2+}$. The isomerization characteristics of *cis,mer*-[Re(CO)$_2$(κ^1-dpm)(κ^2-dpm)X]$^+$ are not known because of the rapid formation of *cis,mer*-[Re(CO)$_2$(κ^1-dpmO)(κ^2-dpm)X]$^+$, but it is interesting that both this cation and *cis,mer*-[Re(CO)$_2$(κ^1-dpmMe)(κ^2-dpm)X]$^+$ do not isomerize on the voltammetric time scale, and analogous reactivities are observed for the ape complexes.

The binuclear manganese complexes *cis,fac*-{Mn(CO)$_2$(dpe)X}$_2$(μ-dpe) are arguably the most interesting compounds discussed in this paper. The stability of the singly and doubly oxidized binuclear complexes is remarkable when compared with those derived from the isoelectronic chromium complex *mer,mer*-{Cr(CO)$_3$(dpe)}$_2$(μ-dpe). In that system, the monocation is stable on the synthetic time scale only at −78 °C, while the dication is stable only on the voltammetric time scale at that temperature.[19] The oxidized manganese dinuclear compounds are not only stable at room temperature, but each half of the molecule is well behaved (almost independent of the other) in its isomerization properties. In contrast, while the rhenium complexes have notable stability for the oxidized species, they do not seem to rapidly isomerize upon oxidation.

Acknowledgment. We gratefully acknowledge the Australian Research Council for financial support. J.N.W. thanks the Australian Commonwealth Government for a Post Graduate Research Award.

Supporting Information Available: Figures S1−S7, containing NMR spectra. This material is available free of charge via the Internet at http://pubs.acs.org.

OM034388T

---

(23) Colton, R.; Dakternieks, D. *Inorg. Chim. Acta* **1993**, *208*, 173.

(24) Colton, R.; Harvey, J.; Traeger, J. C. *Org. Mass Spectrom.* **1992**, *27*, 1033.